

Robustness Analysis of the European Air Traffic Network

Mr. Kuang-Chang Pien

Imperial College London, Department of Civil and Environmental Engineering, Centre for Transport Studies, South Kensington Campus, Skempton Building, SW7 2AZ London United Kingdom

Email: k.pien11@imperial.ac.uk

Phone: +44(0) 2075942705

Corresponding author: Dr. Ke Han

Imperial College London, Department of Civil and Environmental Engineering, Centre for Transport Studies, South Kensington Campus, Skempton Building, SW72AZ London United Kingdom

Email: k.han@imperial.ac.uk

Phone: +44(0) 2075945682

Mr. Wenlong Shang

Imperial College London, Department of Civil and Environmental Engineering, Centre for Transport Studies, South Kensington Campus, Skempton Building, SW72AZ London United Kingdom

Email: wenlong.shang12@imperial.ac.uk

Phone: +44(0) 7521549645

Dr. Arnab Majumdar

Imperial College London, Department of Civil and Environmental Engineering, Centre for Transport Studies, South Kensington Campus, Skempton Building, SW72AZ London United Kingdom

Email: a.majumdar@imperial.ac.uk

Phone: +44(0) 20 7594 6037

Prof. Washington Ochieng

Imperial College London, Department of Civil and Environmental Engineering, Centre for Transport Studies, South Kensington Campus, Skempton Building, SW72AZ London United Kingdom

Email: w.ochieng@imperial.ac.uk

Phone: +44 (0)20 7594 6100

34 Abstract

35 The European Air Traffic Network (ATN), comprising of a set of airports and Area
36 Control Centres (ACCs), is highly complex. The current indicator of its performance, *air*
37 *traffic flow management* (ATFM) delays, is insufficient for planning and management
38 purposes. Topological analysis of air traffic networks of this kind has highlighted *Betweenness*
39 *Centrality* (*BC*) as an indicator of network robustness, although such an indicator assumes no
40 knowledge of actual traffic flows and the network's operational characteristics. This paper
41 conducts topological and operational analyses of the European ATN in order to derive a more
42 relevant and appropriate indicator of robustness. By applying a flow maximisation model to
43 the network influenced by a range of capacity reductions at the local level, we propose a new
44 index called the *Relative Area Index* (*RAI*). The *RAI* quantifies the importance of an
45 individual node to the performance of the entire network when it suffers from capacity
46 reduction at a local scale. Air traffic data from three typical busy days in Europe are utilised
47 to shown that the *RAI* is more flexible and capable than *BC* in capturing the network impact
48 of local capacity degradation. This index can be used to assess network robustness and
49 provide a valuable tool for airspace managers and planners.

50 Keywords

51 Air traffic network; robustness; capacity; linear programming

52

53 1. Introduction

54 High air traffic demand in Europe in recent decades has resulted in the severe
55 congestion experienced at both busy airports and en-route airspace. The latter is controlled by
56 Area Control Centres (ACCs). Such congestion has not only caused severe delays and
57 detrimental environmental impacts, but also posed threats to the safety of air travel.
58 Furthermore, with annual air traffic demand in Europe forecast to increase by 2.5 % between
59 2015 and 2021 (EUROCONTROL, 2015), it is expected that the current capacity of the
60 European air transport network will be simply insufficient to cope with this increase. The
61 capacities of ACCs and airports can be defined in terms of maximum number of flights that
62 can be handled in a given period of time.

63 Compounding this problem of a shortage of capacity on the network is the uneven
64 distribution of air traffic in Europe. According to the Network Operations Report 2013, the
65 top twenty busy airports and congested ACCs were responsible for 67% of all Air Traffic
66 Flow Management (ATFM) delays in 2013 (EUROCONTROL, 2014).

67 In order to ameliorate these negative effects and to improve airspace capacity, the
68 Single European Sky (SES) Air Traffic Management (ATM) Research (SESAR) program
69 was launched and one of its features is to change the ATM of Europe from a local to a
70 network level. SESAR envisages that European airspace will be managed as a continuum and
71 as a consequence, network capacity becomes one of the most important Key Performance
72 Areas (KPA). This move to a network level operation and management means that it is
73 essential to understand the fundamental characteristics of the Air Traffic Network (ATN),
74 especially the connections (i.e. the “connectivity”) between elements of the network. The
75 mathematical science of topology, which is concerned with network characteristics, provides
76 a viable method for assessing the characteristics of the European ATN. In addition to the
77 topological characteristics, the importance of each constituent node relative to the operation
78 of the entire ATN, in terms of capacity, flow, and bottleneck, needs to be investigated in
79 order to understand their roles and impact in the events of network deterioration or
80 expansion. This paper applies complex network theory, robustness analysis, and network
81 optimization to offer insights on the topological and operational characteristics of the
82 European ATN and provide a quantifiable measure of the importance of its constituent nodes
83 when the network suffers from local distress.

84 An ATN can be represented by a set of nodes and links. Conventionally, these nodes
85 can be waypoints, en-route airspace or airports, and the links are the flight routes, between
86 these nodes, e.g. airways in en-route airspace. The European ATN is a nonlinear, dynamic
87 and complex system that comprises of numerous heterogeneous components and stakeholders
88 such as airports, Air Traffic Control (ATC) and airspace users. In addition to the
89 heterogeneity of the components, the operational concepts and interactions between different
90 components make ATNs difficult to analyse. Initial studies on the ATNs tend to focus on
91 their topological characteristics, through complex network theory (Holmes, 2004).
92 Comprehensive reviews of existing studies on the application of complex network theory to
93 air transport networks are provided by Sun et al. (2014) and Sun and Wandelt (2014); they
94 found that these studies focus on airports and cities but failed to consider en-route airspace
95 (Lordan et al., 2014; Wei et al., 2014; Zhao et al., 2014). Therefore, Sun et al. (2014)
96 conducted topological analysis on the ATNs in 15 countries, including the USA and major
97 European nations, in which the constituent nodes are both airports and en-route waypoints
98 and the links are flight routes between the nodes. Five topological indices namely: degree,
99 distance strength, Weighted Betweenness Centrality (hereafter referred to as betweenness
100 centrality or *BC*), weighted closeness centrality and edge length distribution were calculated.
101 The authors suggest that *BC*, originally proposed by Freeman (1979), can serve as an index
102 of network robustness and indicates the number of shortest paths passing through a given

103 node. A node with high BC is used by more flights and the capacity of it is consequently
104 saturated earlier. Therefore, a network is considered more robust against capacity-reduction
105 at nodes when the network contains nodes with a smaller BC compared to other nodes.
106 However, this conclusion is solely based on topological characteristics and is not validated by
107 using the relevant data of air traffic.

108 In response to the lack of a suitable robustness index that captures the operational
109 aspect of an ATN, this paper proposes a new index, namely the Relative Area Index (RAI), to
110 assess network robustness based on the actual flight data from three of Europe's busiest days
111 and the published capacity of airports and ACCs. The RAI is developed based on the change
112 in the maximum network flows, calculated through a linear programming (LP) approach,
113 caused by a range of capacity reductions at a given node. Such capacity degradation may be
114 due to local disruptions such as meteorological influence and industrial action. The LP
115 approach is significant in that it provides a theoretical upper bound on the network flow,
116 while taking into account the capacity reduction that occurs at its constituent nodes.
117 Moreover, the estimated maximum flow on each node is significantly correlated with the
118 empirical maximum flow on congested days. Therefore, the LP-based maximum network
119 flows can reasonably reflect the network capacity of the European ATN.

120 This LP approach, along with the European ATN data that it relies on, are developed
121 using flight profile data provided by the European Organisation for the Safety of Air
122 Navigation (EUROCONTROL). The data were collected on a typical busy day in 2012. This
123 paper extends the analyses of Sun et al. (2014) and Pien et al. (2014) by comparing BC with
124 the new network robustness index (RAI) for the European ATN. The latter index takes into
125 account a range of capacity reduction and its impact on the network operation, rather than
126 simply removing the node, and thus is more realistic in characterizing the robustness of the
127 ATN.

128 This paper not only calculates the topological index (betweenness) of the entire
129 European ATN for the first time in the literature, but also provides a validated tool (RAI) for
130 Europe's airspace managers and planners to assess network robustness in the event of any
131 local deterioration of nodal capacity. The RAI is compared with the actual traffic demand and
132 published capacity at each node and shown to have the potential to identify the important
133 nodes in the network.

134 The rest of this paper is organised as follows. Section 2 introduces an overview of
135 robustness analysis in transport networks and relevant literature. The development of the
136 RAI is also introduced. The European ATN flight profiles, capacity constraints, and network
137 structures are described in detail in Section 3. Section 4 presents the linear programming
138 approach for traffic flow maximisation. Section 5 presents the results and analysis on the
139 European ATN. The findings are discussed in Section 6 prior to the conclusions in Section 7.

140 **2. Robustness Analysis**

141 Since the definition of robustness varies in different fields, it is pertinent to review the
142 definitions and their context in the literature to define the robustness of an ATN.
143 Furthermore, the current *Key Performance Indicator* (KPI) of network capacity in the
144 European ATN is introduced. Based on previous research, the conventional index of BC is
145 described. Finally, we develop a new index, the RAI , to assess the robustness of the European
146 ATN.

147 **2.1. Literature review**

148 The robustness of transport networks has been a central focus of network planning
149 and management. It is often investigated in different performance areas such as stability,

150 resilience and permanence to assess the capability of handling worsened or perturbed
151 conditions of the network.

152 Since there are numerous categories of networks, there is no universal definition of
153 network robustness, though the following three are highly relevant for this paper:

- 154 • “*The degree to which a system or component can function correctly in the presence of*
155 *invalid inputs or stressful environmental conditions*” (Geraci et al., 1991).
- 156 • “*The degree to which a system is capable of functioning according to its design*
157 *specifications in the case of serious disruptions*” (Immers et al., 2004).
- 158 • The robustness of an electrical network is defined as *the capability of maintaining its*
159 *structure and function when the network is exposed to perturbations* (Holmgren, 2007)

160 Given these definitions, the robustness of a given system or component is therefore
161 the capability of maintaining its function or performance in order to cope with disruptions,
162 perturbations and stressful conditions. Whilst useful, these studies focus on either an
163 individual system or a component. In order to cope with the robustness at network level, it is
164 illustrative to consider the experience of research on transport networks as outlined below.

- 165 • Sakakibara et al. (2004) proposed a topological index to evaluate the depressiveness and
166 concentration of road networks in the presence of disasters. They suggested that a
167 network is considered robust when it is able to minimize the isolation of districts when
168 catastrophic disasters occur.
- 169 • Scott et al. (2005) proposed the Network Robust Index (NRI) to identify the critical links
170 of a highway network. This index was calculated by comparing the changes in travel time
171 cost of the network when a given highway segment (i.e., network link) is removed from
172 it. Compared to the conventional method of using the ratio of volume to capacity which
173 can only reflect the congestion at local level, the NRI provides better planning solutions
174 to enable the identification of critical links at the network level.
- 175 • Nagurney and Qiang (2007a) proposed a network efficiency measure to assess the
176 efficiency of congested networks. Their approach is used to rank the importance of a
177 given link by comparing the change of total travelling costs when the link is removed
178 from the network. In their later work Nagurney and Qiang (2007b) use the relative change
179 of network efficiency as an index to assess network performance when the capacities of
180 all links are reduced by the same percentage. The authors therefore developed the
181 Relative Total Cost Index (RTCI) to assess the robustness of networks against a global
182 decrease of link capacities (Nagurney and Qiang, 2009). Compared to removing links
183 from the network, this approach provides a more realistic method of assessing network
184 robustness when disturbance occurs on any of its constituent components.

185 Based on these studies, the robustness of a network can be defined as the capability of
186 maintaining network performance while its functioning components, namely nodes and links,
187 are under stress. With this definition in mind, we conduct robustness analysis by taking into
188 account the topological and operational characteristics of the European ATN, and treating
189 network capacity as the main *key performance area* (KPA). In particular, we consider the
190 *maximum network flow*, which is obtained through an optimization procedure, as the key
191 indicator of network capacity. Accordingly, the robustness of the European ATN in this paper
192 is related to the capability of delivering the maximum traffic flows against degradation of
193 nodal capacities. In the following sections, the current KPIs of network capacity and the
194 conventional index of network robustness are reviewed.

195 **2.2. KPI of network capacity: ATFM delays**

196 Currently, ATFM delays are used as the KPI to monitor network capacity
197 (EUROCONTROL, 2007). This is the duration between the last take-off times requested by
198 the aircraft operator and the take-off slots allocated by the central flow management unit

199 namely the Network Manager Operations Centre. This duration follows an air traffic flow
 200 regulation, which is subsequently communicated by the flow management positions to an
 201 airport or en-route centre.

202 However, there is a major deficiency with this measure since ATFM delay is not a
 203 direct measure of capacity but rather is a proxy that reflects the extra time caused by capacity
 204 shortages, which are in turn caused by various factors at airports and in en-route airspace.
 205 Since it is an indirect measure, there is an inherent inaccuracy in identifying the important
 206 nodes in a network. For instance, Maastricht ACC highlights the limitation of ATFM delays
 207 as an indicator. Although the air traffic demand in Maastricht ACC is amongst the highest in
 208 Europe, the ATFM delays are relatively low. However, since the nodes with high ATFM
 209 delays are considered as bottlenecks in the European ATN, we use them to conduct an
 210 intuitive verification of the other indices.

211 **2.3. Topological Index: Betweenness Centrality (BC)**

212 In complex network theory, nodes within a network may be ranked by using different
 213 centrality measures (Wasserman, 1994). The rank of a given node reflects the measurement
 214 of some particular structural property in the network. Several centrality measures, such as
 215 degree, betweenness, and closeness, can be used to rank the importance of nodes, among
 216 which betweenness is the most widely used as an index of network resilience and robustness
 217 (Holme et al., 2002; Newman, 2001). The betweenness centrality (BC) of a node is defined as
 218 the probability that it lies in the shortest path(s) between all origin-destination (OD) pairs
 219 (Dehmer, 2011; Di Paolo et al., 2011). Mathematically, the conventional formulation of BC
 220 can be presented as:

221

$$BC_i = \sum_{m,n \in v} \frac{S_{mn}^i}{S_{mn}} \quad (1)$$

222

223 where BC_i is the betweenness of the node i . S_{mn} is the total number of shortest paths between
 224 any pair of nodes (m, n) and S_{mn}^i is the number of shortest paths passing through the node i .

225 Newman (2001) states that the higher the BC , the more influential is the node. The
 226 largest increase in the travel distance among nodes occurs when the node with the highest BC
 227 is removed. This explains intuitively the importance of high- BC nodes relevant to the overall
 228 performance of the network. In addition, a network with many low- BC nodes is more robust
 229 than that with many high- BC nodes. Brandes (2001) notes that BC is the most frequently
 230 employed centrality index in the analysis of social networks; and it is mostly based on
 231 shortest paths. Barrat et al. (2004) claim that nodes in the inner network are more likely to be
 232 used by shortest paths than those in the outer network. Therefore, in an ATN, it can be
 233 intuitively assumed that the airspace nodes are more likely to be passed by the shortest paths
 234 and the nodes with high BC are more likely to handle more traffic, when the traffic demands
 235 are uniformly distributed. Travellers within a network tend to choose the shortest paths and as
 236 a result, the nodes with high BC tend to be used by more travellers.

237 However, in the ‘real world’ of transport operations, nodes with high BC are not
 238 necessarily busy (or heavily loaded) due to the fact that the traffic network flows are jointly
 239 determined by a number of factors such as travel demand distribution, complex decision
 240 factors, and route choice patterns that are not based on shortest paths (i.e., not all-or-nothing
 241 assignment). For example, Cats and Jenelius (2014) developed a dynamic-stochastic model to
 242 evaluate the impacts of disruptions, and demonstrated that BC may not be a good indicator of
 243 link importance in a road network. Guimera and Amaral (2004) modelled a world-wide
 244 airport network and showed that the airports with high BC are not necessarily hubs. They

245 argued that geo-political constraints play an important role in the growth of airport networks
 246 and other critical infrastructure. In addition, although both are modelled as nodes in an ATN,
 247 the roles of airports and ACCs are different. An airport not only acts as an origin/destination
 248 but also as a transfer node (hub), which means that it serves as the en-route node of a
 249 complete trip from the origin to the destination. However, the conventional formulation
 250 shown in (1) treats the airports and ACCs equally without considering their heterogeneity.
 251 Therefore, this conventional BC needs to be tailored and improved to accommodate the
 252 unique characteristics of the ATN. All these aforementioned factors contribute to the
 253 consensus that BC may no longer be sufficient to assess the robustness of a complex network
 254 such as the ATN. This paper contributes to this line of research by proposing the relative area
 255 index (RAI), which serves as an alternative robustness index that captures the ATN's flow
 256 capacity and certain aspects of its operational features.
 257

258 **2.4. Relative Area Index (RAI)**

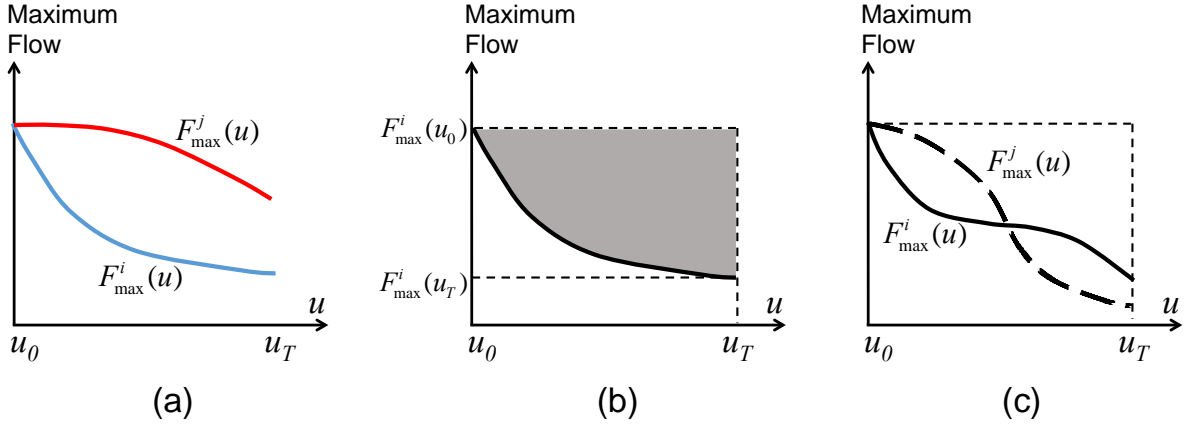
259 Built upon the definition of robustness, the *RAI* assesses and quantifies the impact on
 260 the maximum network flow of a wide range of capacity reductions that occur at a local
 261 (nodal) level. Its derivation is outlined below.

262 The potential reduction of nodal capacity in the ATN is parameterised with u , which
 263 is termed the *degradation parameter (DP)*. We employ the notation $F_{max}^i(u)$ to represent the
 264 maximum network flow when a capacity reduction expressed by u is applied to node i . The
 265 procedure of finding the maximum network flow with a given degradation parameter
 266 amounts to a linear program, as we describe in detail later in Section 4.

267 In this study, two types of *DPs* are considered: (1) percentage based *DP*; and (2)
 268 absolute value based *DPs*. The Percentage-*DP* (u^P) ranges from 0% to 100%, and represents
 269 the reduction of the subject node's capacity in percentage. The Absolute-*DP* (u^A) ranges
 270 from 0 to 50 (in flights per hour). The value 50 is chosen since it is about half of the capacity
 271 of the node with the smallest capacity (LA PALMA airport). Anything significantly larger
 272 than 50 may cause the reduced capacity at some nodes to be negative, which is clearly
 273 infeasible. In order to distinguish these two methods of capacity reduction, we denote the *RAI*
 274 based on Percentage-*DPs* by RAI_P , and the *RAI* based on Absolute-*DPs* by RAI_A .
 275

276 Since the network maximum flow problem is formulated as an optimization problem
 277 constrained by nodal capacities, we deduce that $F_{max}^i(u)$ is a monotonically decreasing
 278 function of u , where a larger u represents greater capacity degradation at the relevant node.
 279 **Error! Reference source not found.** illustrates the rationale behind *RAI*. As shown in
 280 **Error! Reference source not found.**(a), two functions, $F_{max}^i(u)$ and $F_{max}^j(u)$ corresponding
 281 to nodes i and j respectively, indicate that node i is the more important one as far as
 282 maximum network flow is concerned. This is because the same level of degradation yields a
 283 smaller network flow when applied to node i than node j . In general, the lower the function
 284 $F_{max}^i(u)$, the more detrimental it is to reduce the capacity at node i . In order to further
 285 quantify such an observation, we consider the area formed by the graph of $F_{max}^i(u)$, the
 286 vertical line passing through u_T , and the horizontal line passing through $F_{max}^i(u_0)$. Such an
 287 area is illustrated as the shaded part in **Error! Reference source not found.**(b). It is
 288 understood that the large the area, the more critical is the node. For an ATN, the more critical
 289 nodes there are, the less robust is the network against capacity reductions. Finally, we note
 290 that two distinct functions may yield the same area, as shown in **Error! Reference source**
 291 **not found.**(c). Thus, in order to distinguish such circumstances, we introduce the *weighting*
 292 *parameters* (WP) $w(u)$. The WPs assigns different priorities to different range of capacity
 293 reductions, and may depend on the node of interest, type and nature of capacity reduction,

294 and application scenarios. For example, if the main cause of capacity reduction is scheduled
 295 maintenance, which has a mild effect on airport capacity, then lower values of u will be
 296 assigned higher weights. Therefore, in **Error! Reference source not found.**(c) the node i
 297 (solid line) corresponds to larger weighted area than node j (dashed line), and thus is more
 298 critical.
 299



300 (a) (b) (c)
 301 Figure 1. Illustration of the relative area index.

302
 303 In this study, we select three types of WPs. The first type assumes equal weights for
 304 all values of the degradation parameter $u \in [u_0, u_T]$. The second type of WP assigns higher
 305 weights to small values of u , in contrast to the third type, which assigns lower weights to the
 306 small values. By using these three sets of WPs, it is possible to gain insights into the (global)
 307 influence of the local capacity-reductions. With this in mind, we formulate the *relative area*
 308 *index (RAI)* for a given node i as:
 309

$$RAI^i = \frac{\int_{u_0}^{u_T} w(u)(F_{\max}^i(u_0) - F_{\max}^i(u))du}{\int_{u_0}^{u_T} w(u)F_{\max}^i(u_0)du} \quad (2)$$

310
 311 We note that a normalisation factor (denominator) is applied to the aforementioned weighted
 312 area (numerator). As we previously mentioned, percentage-based and absolute-value-based
 313 degradation parameters (u^P and u^A) are considered; namely, $u^P \in [0, 1]$ and $u^A \in [0, 50]$.

314 In general, the *RAI* defined for a given node encapsulates the global impacts of
 315 capacity reductions at this node, which depend not only on the network topology, but also on
 316 the configuration of OD pairs, flight routes, and nodal capacities. The *RAI* is defined in terms
 317 of a flow maximisation problem, and is not available in a closed form. Thus, it is difficult to
 318 predict the distribution of *RAIs* using simple topological indicators such as *BC*. There are,
 319 however, a few simple interpretations of the *RAI*. In particular, it is reasonable to expect that
 320 nodes with higher capacities should in general have larger (percentage-based) RAI_P values
 321 than those with lower capacities based on the following observation: the percentage-based
 322 capacity reduction at a high-capacity node results in greater absolute reductions. However, as
 323 we subsequently show in Section 5.2, some nodes in the European ATN possess RAI_P that
 324 are quite counter-intuitive, as suggested by their size, capacity, and significance to the
 325 network.

326 **3. The European Air Traffic Network**

327 The key elements required to conduct the robustness analysis are the weighted
 328 adjacency matrix and the maximum network flow estimation method. The former is used to
 329 calculate betweenness, while the latter is used to calculate the *RAIs* for the network against
 330 the capacity reductions at every node. This section introduces the European ATN and the
 331 required data for calculating BC and the maximum network flows.

332 **3.1. Data processing**

333 According to the latest European Network Operations Plan (EUROCONTROL,
 334 2014), the European ATN comprises of 41 countries, and the en-route airspace of Europe is
 335 controlled by 64 ACCs. In order to monitor the air traffic at the network level,
 336 EUROCONTROL records detailed daily profiles of all flights in Europe at the levels of the
 337 ACCs, en-route sectors and waypoints – the latter of which are often associated with
 338 navigation aids, in particular radars. Each flight profile represents a flight route that uses a
 339 sequence of nodes. This dataset provides the information on the times and coordinates of
 340 each flight at every node. In order to investigate the robustness at the network level, airports
 341 and ACCs are employed as the constituent nodes of the European ATN.

342 Flight profiles recorded on 1st July 2012 were used to extract the required information.
 343 On this day, a total of 28,904 flights were scheduled, among which 28,885 flight profiles
 344 were recorded by the radars. In total, 28,753 flight profiles are used for this study, with the
 345 remainder excluded since they either used unrecognized airports or passed through
 346 unrecognized airspace.

347 The average ATFM delays per flight on this particular day were among the highest in
 348 2012. This date also falls within the European summer, which is the season with the highest
 349 traffic demand throughout a year. The advantage of using the flight profiles for this day is
 350 that the high ATFM delays enable us to capture the spatial configuration of traffic
 351 congestion, while the high traffic demands (flight routes) provide sufficient information on
 352 the connectivity between nodes. The ATFM delay data are provided by EUROCONTROL.

353 **3.2. Network topology**

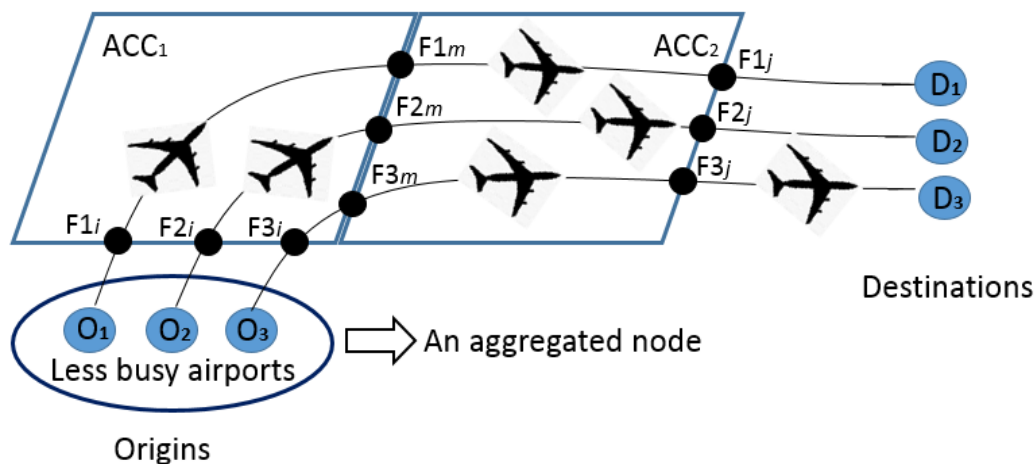
354 The European ATN can be represented as a directed graph, in which the nodes
 355 represent airports and ACCs. A critical notion is connectivity, which can be defined as a
 356 binary state that exists between any two nodes in the network, taking a value one if the two
 357 nodes are connected by a link and zero otherwise. Unlike many traditional transport
 358 networks, the capacity constraints in an ATN are imposed at the nodes (airports and ACCs)
 359 rather than on the links. The declared capacities at airports and en-route airspace are applied
 360 to prevent the relevant node from overload through the mechanism of air traffic flow
 361 management (ATFM), which includes re-routing and the imposition of flow regulation. Air
 362 traffic at European airports and in en-route airspace is required to comply with the declared
 363 capacities. Based on these characteristics, the European ATN can be regarded as a
 364 capacitated transport network and, consequently the traffic flows within it cannot exceed the
 365 theoretical maximum. The fundamental components of a capacitated transport network are
 366 the constituent nodes and links, as detailed below. These components can be updated and re-
 367 selected by using different techniques with the latest operational reports when they are
 368 available.

369 **3.2.1. Constituent nodes**

370 Based on the flight profiles, this network consists of 850 nodes, which include 784
 371 airports, 64 ACCs and two external nodes. The external nodes are used to represent airports
 372 and airspaces that are external to the European region. According to Pien et al. (2014), the

373 airports can be categorized as ‘busy airports’ and ‘less busy airports’. A total of 67 busy
 374 airports were selected based on the top airports listed in EUROCONTROL (2013c) and
 375 EUROCONTROL/FAA (2009). These busy airports carry about 60% of the overall flights in
 376 Europe, while the less busy airports carry the remaining 40%.

377 The capacity data at less busy airports are not publically available. In order to
 378 overcome this difficulty, we treat the less busy airports collectively as one or several
 379 aggregate nodes. Figure 2 shows the method of creating an aggregate node that represents a
 380 group of less busy airports that are of interest to a particular ACC. The connectivity among
 381 these less busy airports and relevant ACC is identified through the flight profile data. It is
 382 worth noting that some less busy airports may be adjacent to more than one ACC. In this
 383 case, we assign this airport to the ACC that contains the most number of flights originating
 384 from it. Following this rule, we are able to assign each less busy airport to a unique ACC; and
 385 less busy airports assigned to the same ACC are aggregated to form an aggregate node. By
 386 using the aggregate nodes, the issue of unknown capacities of the less busy airports is
 387 circumvented since active bottlenecks can occur only at the level of ACCs that watch over
 388 the less busy airports, rather than at these airports themselves; in other words, the capacities
 389 of individual less busy airports are not explicitly needed for the flow maximization problem.
 390 Applying the aggregate nodes also reduces the network size while maintaining the
 391 connectivity between the less busy airports and their adjacent ACCs. The reduced network
 392 contains 197 nodes, including 67 busy airports, 64 aggregate airports, 64 ACCs and 2
 393 external nodes.



394
 395

Figure 2. Illustration of the aggregate airports.

396 The flow maximization problem we shall consider later employs a static flow
 397 modelling approach; that is, we consider the stationary flows in the network on a daily basis,
 398 without explicitly considering the within-day dynamics of various variables. Thus, the
 399 capacities of the airports and ACCs (in flights per day) as we consider in this paper are
 400 calculated from the declared capacity (in flights per hour) by a multiplication factor of 16 and
 401 24, respectively, meaning that the operational hours at the airports and ACCs are 16 hours
 402 and 24 hours per day. Although the air traffic demand and traffic intensity are unevenly
 403 distributed over the duration of operational hours, the static modelling approach for ACCs
 404 and airports enables the calculation of the theoretical maximum network flows, which can
 405 serve as a theoretical upper bound of network capacity.

406 3.2.2. Constituent links

407 A directional link in the network is defined as the connectivity between an ordered
 408 pair of nodes. The link between any pair of nodes is established if the flight profile data

409 suggests the consecutive passing of the two nodes by at least one flight. The weight of the
 410 link is defined to be the average flying distance from its tail node to its head node, which is
 411 obtained using the actual flight data.

412 Issues arise from the different spatial characteristics of airports and ACCs. In
 413 particular, an airport can be regarded as a single point with negligible size while an ACC
 414 usually covers a significantly larger area. The distance between an airport (or an aggregated
 415 airport) to its adjacent ACC can be calculated by averaging the distance between the airport
 416 and the entry point to its adjacent ACC, and such entry points are recorded in the dataset of
 417 flight profiles.

418 However, the flying distance between two ACCs cannot be directly calculated by
 419 using the distance between their centres, due to their relatively large areas and irregular
 420 shapes (ACC boundaries in Europe follow national borders). Assuming that N flights are
 421 flying through node i and j , the flying distances of these N flights between the node i and j are
 422 $D_{(i,j)}^N$. The weight of the link between ACC_i and its adjacent ACC_j ($L_{(i,j)}$) can be formulated
 423 as:

424

$$L_{(i,j)} = \frac{1}{2N} \sum_{N=1}^N D_{(i,j)}^N \quad (3)$$

425 3.2.3. Validity of the network data

426 As mentioned earlier, the network topology and the flow maximization problem are
 427 based on the flight data on 1st July 2012. Datasets collected on two additional busy days,
 428 namely 28th and 29th July 2012, are used to validate the network data. More specifically, we
 429 use correlation coefficients to assess the similarity of the network adjacency matrices
 430 calculated from the data on these three days. On the other hand, the Mean Absolute
 431 Percentage Error (MAPE) and correlation coefficients are used to compare the maximum
 432 flows (details to follow in Section 4) calculated by using data on these three days.

433 The correlation coefficients for the network adjacency matrices on the three days are
 434 above 0.85. In addition, the correlation coefficients among the maximum flows on these three
 435 days are above 0.99 and the MAPEs are less than 0.5%. This shows consistency of our data-
 436 processing method and the validity of the resulting network topological information and
 437 maximum flow data.

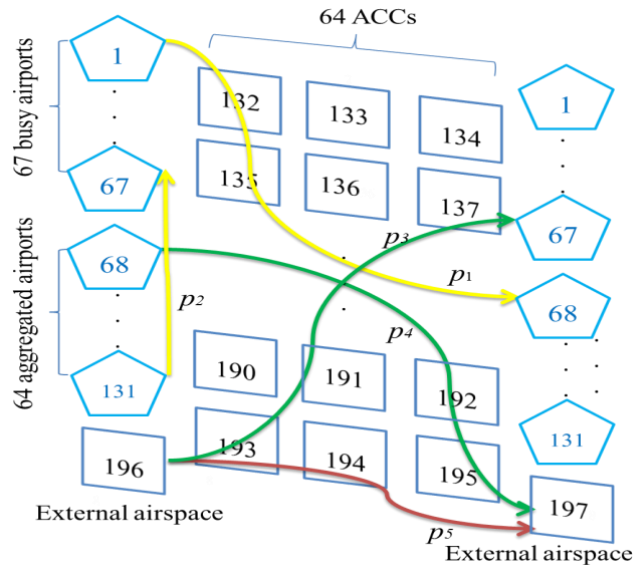
438 4. Traffic Flow Maximization

439 The problem of finding the theoretical maximum network flow subject to the network
 440 topology and capacity constraints is formulated as a linear program. In this section, we first
 441 recap the LP approach for maximising network flows originally proposed by Pien et al.
 442 (2014). This is followed by an interpretation of the *RAI* in relation to the Lagrange
 443 Multipliers (LM), which is relevant to the linear program and the marginal costs of local
 444 capacity reduction.

445 4.1. Network flow maximisation formulated as a linear program

446 As mentioned earlier, the European ATN is considered as a capacitated transport
 447 network in which the operations at airports and in ACCs are subject to their individual
 448 capacity limits. The maximum network flows are estimated by using a LP approach. The
 449 estimated maximum flow on each node is significantly correlated to the empirical maximum
 450 flow on congested days. Therefore, the estimated maximum network flows can reasonably
 451 reflect the network capacity of the European ATN.

452 Figure 3 depicts the structure of the network and the flight paths therein. The network
 453 comprises of busy airports, aggregated airports and ACCs. An aircraft departs from its origin
 454 airport and flies along its flight path in en-route airspace to its destination airport. The flights
 455 that use European airspace can be categorised into three groups: intra-Europe flights, inter-
 456 continental flights, and over-flights. The flights flying along the flight paths p_1 and p_2 are
 457 intra-Europe flights that fly between two European airports. The flights along paths p_3 and p_4
 458 are inter-continental flights that fly from an European airport to an airport outside Europe or
 459 vice versa. The group of over-flights p_5 represents the flights passing European airspace
 460 without using any European airports.
 461



462
 463 Figure 3. Structure of the European ATN.

464 We consider a network with given sets of paths (P) and origin-destination (OD) pairs
 465 (W). For any $(i, j) \in W$ where i denotes origin and j denotes destination, let P_{ij} be the set of
 466 flight paths connecting i to j . Each flight path is represented as a set of nodes (airports and
 467 ACCs) it traverses. The relationship between paths and nodes is encapsulated by the path-
 468 node incidence matrix (δ_{pv}):
 469

$$\delta_{pv} = \begin{cases} 1 & \text{if } v \in p \\ 0 & \text{otherwise} \end{cases} \quad (4)$$

470 where v denotes a node, and p denotes a path. In addition, each node v in the network has a
 471 flow capacity C_v .

472 The maximum network flow problem is formulated as follows. The objective is to
 473 maximize the path-based flows in the entire network:
 474

$$\max \sum_{p \in P} f_p \quad (5)$$

475 where f_p denotes the flow along path p . The constraints include:

476 Flow capacity constraint: $\forall k \in \mathcal{AN}$ (the set of nodes)

$$\sum_{p \in P} \delta_{pk} f_p \leq C_k \quad (6)$$

Nonnegativity: $\forall p \in P(\text{the set of flight paths})$

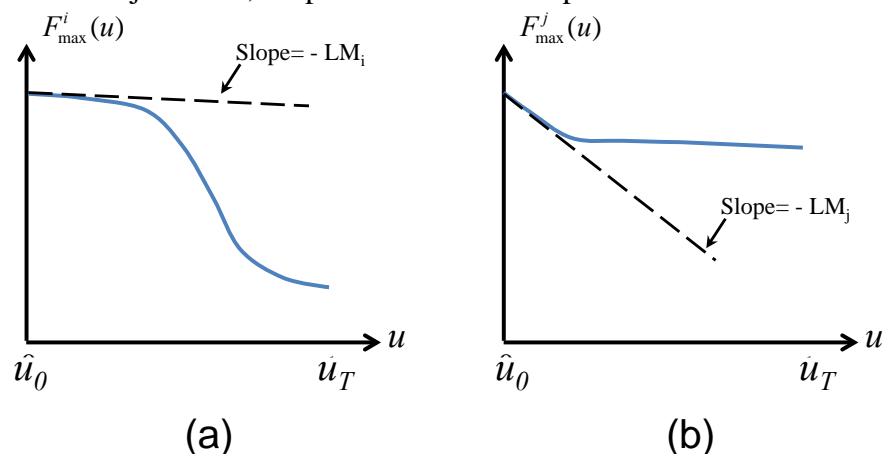
$$f_p \geq 0 \quad (7)$$

477 The influence of capacity reduction at a given node on the maximum network flows can be
 478 obtained by solving a family of such linear programs, each with a decreased flow capacity at
 479 a given node. This procedure is the basis for calculating the *RAI*.

480 4.2. Lagrange multiplier and *RAI*

481 The use of the Lagrange multiplier is a common approach to solving optimization
 482 problems (Jahn, 2007). The Lagrange multiplier is the rate of change of a quantity being
 483 optimized as a function of the constraint variable. In the case of maximizing network flows,
 484 the Lagrange multiplier is the sensitivity of the maximum network flow with respect to the
 485 change in the capacities. It can be interpreted simply as the marginal cost (gain) of the
 486 network maximum flow with respect to an infinitesimal reduction (increase) in the nodal
 487 capacity. Lagrange multipliers are zero at non-bottleneck nodes, which corresponds to the
 488 complementarity conditions arising from duality; this means that small changes in capacity at
 489 these non-bottleneck nodes have no effect on the maximum network flows. The higher the
 490 Lagrange multiplier, the more critical the node is to the overall throughput of the network.

491 The Lagrange multiplier is related to the *RAI*, since the former is precisely the
 492 derivative of the function $F_{max}^i(u)$ evaluated at 0, with a negative sign. However, the *RAI*
 493 presents knowledge of the rest of the function for $u \in (0\%, 100\%]$ or $(0, 50]$ whereas a
 494 Lagrange multiplier only shows the initial trend of the curve when the capacity reduction is
 495 small; see Figure 4 for an example. In Figure 4(a), the initial decrease of the curve $F_{max}^i(u)$
 496 is small, indicating a small Lagrange multiplier. However, as the capacity reduces further, the
 497 maximum network flow drops drastically. In comparison, Figure 4(b) shows a curve with
 498 steeper initial decrease, but which then stabilises for larger u . From this figure, we see that
 499 the Lagrange multiplier and the *RAI* may provide very different information regarding the
 500 importance of the subject node, despite their relationship illustrated above.



501
 502

Figure 4. Relationship between the Lagrange multiplier and the *RAI*

503

504 We see from these simple examples that the *RAI* is a more comprehensive
 505 performance indicator for a node subject to capacity reductions than the Lagrange multiplier,
 506 as the former captures a whole range of capacity reductions. Moreover, the use of

507 appropriately defined weighting parameters, shown in Eq. (2), makes the *RAI* quite flexible in
 508 addressing a target range of capacity reductions, which can be user defined.

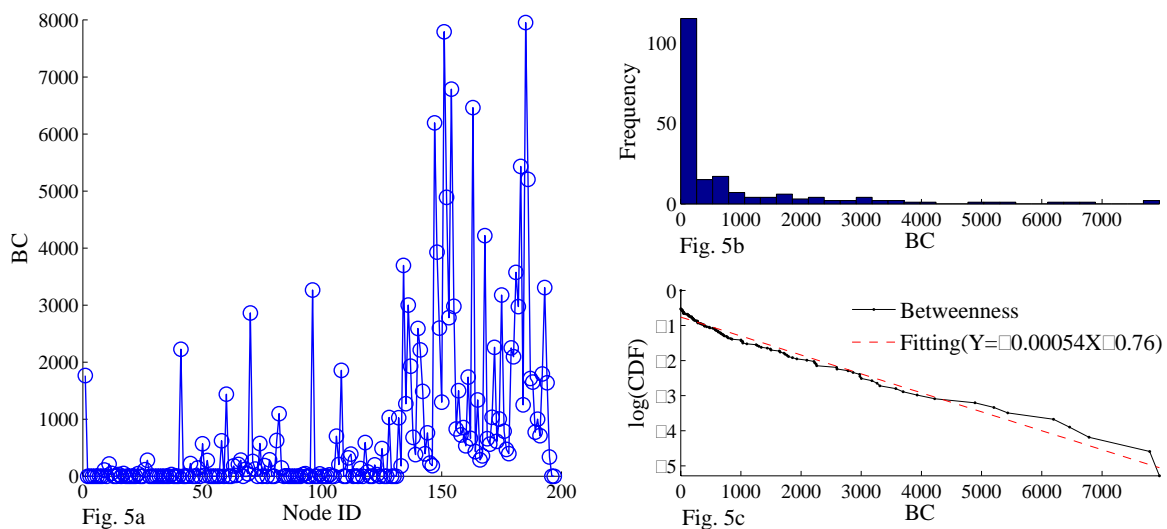
509 5. Results and Analysis

510 In this section, we present results related to the *BC* and *RAI*, and provide some
 511 discussions on their managerial insights in the context of air traffic management on a network
 512 level. Since the focus and the underlying assumptions of *BC* and *RAI* are different, we
 513 compare *BC* to traffic load and *RAI* to nodal capacity. The rationale behind these
 514 comparisons is that nodes with higher *BC* tend to carry more traffic load since most flight
 515 routes follow the shortest paths; on the other hand, nodes with higher capacity are intuitively
 516 more important to the maximum flow of the entire network. In order to simplify our analysis
 517 and to distinguish between airports and airspaces, we extract the top ten airports and
 518 airspaces in each category (*BC* & *RAI*) and highlighting nodes that are significant according
 519 to both the indicators. Since the aggregated nodes are used to maintain the network structure
 520 and do not represent solid locations, we exclude them from the ranking list. The rankings of
 521 the airports and airspaces are then compared with the empirical data on air traffic load, nodal
 522 capacities, and ATFM delays.

523 In subsequent presentation, unless otherwise specified, we assign ID numbers 1- 67 to
 524 the 67 airport nodes, 68 - 131 to the 64 aggregate airport nodes, and 132 - 195 to the 64 ACC
 525 nodes.

526 5.1. Betweenness centrality (BC)

527 Figure 5 displays information of the *BC* in the entire network. Compared to the airport
 528 nodes (ID 1 - 131), the ACC nodes (ID 132 - 195) overall have larger *BC*s. An intuitive
 529 explanation is that the ACC nodes in the network can be considered as inner nodes while the
 530 airport nodes can be regarded as outer nodes (see Figure 3 for an illustration). Thus the inner
 531 nodes tend to have higher *BC*s, an observation consistent with the work of Barrat et al.
 532 (2004).



533
 534 Figure 5. BC in the European air traffic network.

535 Figure 5b and Figure 5c show the histogram and the cumulative distribution function
 536 (CDF) of *BC*s, respectively. The CDF of the weighted *BC* can be fitted by an exponential
 537 function: $P(\geq b) \sim e^{-0.00054b}$. Such a fitting is a common approach in network science to
 538 quantify the robustness of a network based on topological indices such as the *BC*; the reader

539 is referred to Sun et al. (2014) for a more elaborated discussion and more examples of such
 540 fitting for a variety of other air traffic networks.

541

542 The ten airports and airspace with the highest air traffic loads and BCs are listed in
 543 Table 1. It is notable that airport nodes with high BCs do not necessarily have the highest
 544 traffic loads, and vice versa. The airports handling high traffic demands all locate on the
 545 capitals or economic centres rather than the high-BC airports. Therefore, the BC is not
 546 capable to capture the high-traffic airports and this results is consistent with Cats and Jenelius
 547 (2014) and Guimera and Amaral (2004).

548

Rank	Airport		Airspace (ACC)	
	BC	Traffic load	BC	Traffic load
1	VALENCIA	FRANKFURT	GENEVA	LONDON
2	BRUSSELS	PARIS CDG	BREMEN	MAASTRICHT
3	GENEVE	LONDON HEATHROW	<u>MUNICH</u>	KARLSRUHE
4	WIEN SCHWECHAT	SCHIPHOL AMSTERDAM	<u>ROME</u>	<u>MUNICH</u>
5	MAKEDONIA	MADRID BARAJAS	<u>MARSEILLE</u>	<u>MARSEILLE</u>
6	ISTANBUL SABIHA	MUENCHEN	MALMO	<u>ROME</u>
7	TRONDHEIM VAEMES	ISTANBUL ATATURK	ZURICH	LONDON TC
8	CATANIA FONTANAROSSA	ROME/FIUMICINO	<u>LANGEN</u>	<u>PARIS</u>
9	NICE	BARCELONA	AMSTERDAM	<u>LANGEN</u>
10	BIRMINGHAM	PALMA-DE-MALLORCA	<u>PARIS</u>	BREST

549

Table 1. Top ten airports and airspaces that have the highest BCs and traffic loads.

550 In terms of the BCs of airspace (ACC) nodes, five high-BC ACCs, namely Munich,
 551 Rome, Marsellie, Langen and Paris, also handle high air traffic. This result indicates that the
 552 BC is relatively more capable of capturing the important nodes with high traffic demands in
 553 airspace than at airports. However, the corresponding BC-rankings of the top three high-
 554 traffic ACCs, namely London, Maastricht and Karlsruhe are extremely low. Therefore, BCs
 555 cannot fully capture the traffic demands in the real world of operational traffic.

556 5.2. Relative area index (RAI)

557 According to our discussion of the RAI, the capacity of a node may be reduced by a
 558 certain percentage or by an absolute value. The resulting RAI_P and RAI_A , respectively, are
 559 presented and analysed in this section to examine the influence of capacity reductions on the
 560 network capacity. We use Spearman's rank correlation coefficient (r) and p -value (p) to
 561 measure the statistical dependence and the statistical significance between different sets of
 562 results. The detailed results of the RAIs and the BCs, as well as the empirical data, of a
 563 selection of nodes are presented in the Appendix.

564

565 5.2.1. Relative area index with capacity reduction by percentage (RAI_P)

566 In this section, we illustrate three sets of RAI_P over the entire European ATN in Figure
 567 6. These three sets of RAI_P are calculated by using three different weighting parameters that
 568 emphasize the capacity reduction at different levels. The first weighting parameter treats the
 569 importance of capacity reductions at all levels equally, and is indicated as 'Constant' in Figure
 570 6. The second and third weighting parameters assign a low (high) weight to low capacity
 571 reduction and a high (low) weight to high capacity reduction; in particular, they vary the
 572 weight from 0 to 10 and 10 to 0, respectively. Therefore, the second and third weight
 573 parameters emphasize the importance of higher and lower capacity reductions at each node,
 574 respectively.

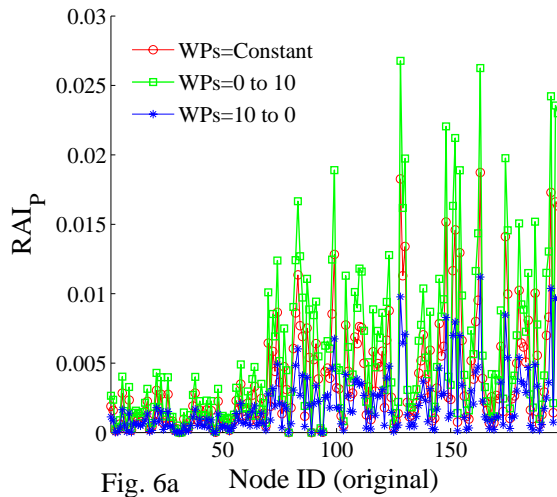


Fig. 6a Node ID (original)

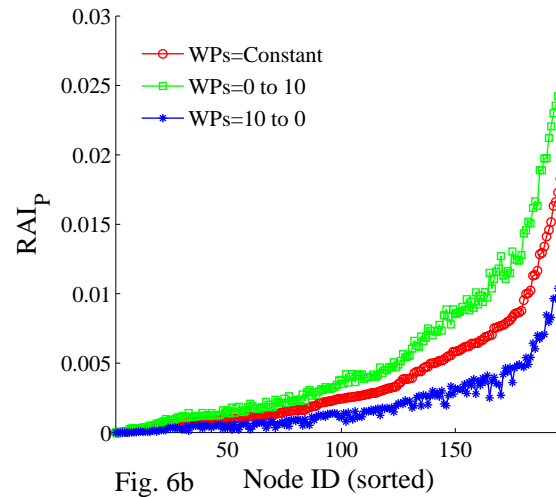


Fig. 6b Node ID (sorted)

575
576
577

Figure 6. RAI_P in the European ATN. Fig. 6b is using new node IDs based on nodes sorted by their RAI_P (with constant weighting parameters).

578 Both the correlation coefficients and Spearman's rank correlation coefficients among
579 these three sets of RAI_P shown in Figure 6 are above 0.97 and the p -values are all close to
580 zero, which indicate that our results attain statistical significance. Moreover, the high
581 Spearman's rank correlation coefficients show that the ranking of nodes based on RAI_P is
582 insensitive to the change of the weighting parameters.

583 Figure 6a also shows that the RAI_P of airports (ID 1 - 67) are generally smaller than the
584 RAI_P of aggregated nodes and ACCs (ID 68 - 195). In view of the fact that airport nodes tend
585 to have lower capacities, this result is in line with the anticipation that the influence of nodes
586 with higher capacities is, in general, larger than those with lower capacities, since the
587 capacity reduction is based on percentages.

588 Table 2 shows that there are five airports and five ACCs with both high RAI_P and high
589 capacities, as appeared in the top ten; they are highlighted in bold. However, the RAI_P and
590 capacity of some ACCs are counterintuitive. For instance, both the traffic load and capacity
591 of London, Maastricht, Karlsruhe and Marseille are high but their RAI_P values are relatively
592 low. In contrast, the RAI_P of Bucharest, Bremen, Madrid, Ankara/Istanbul, Belgrade are high
593 while their capacities are comparatively low. These results imply that the importance of a
594 given node in the presence of capacity reduction is not necessarily in line with its capacity.
595

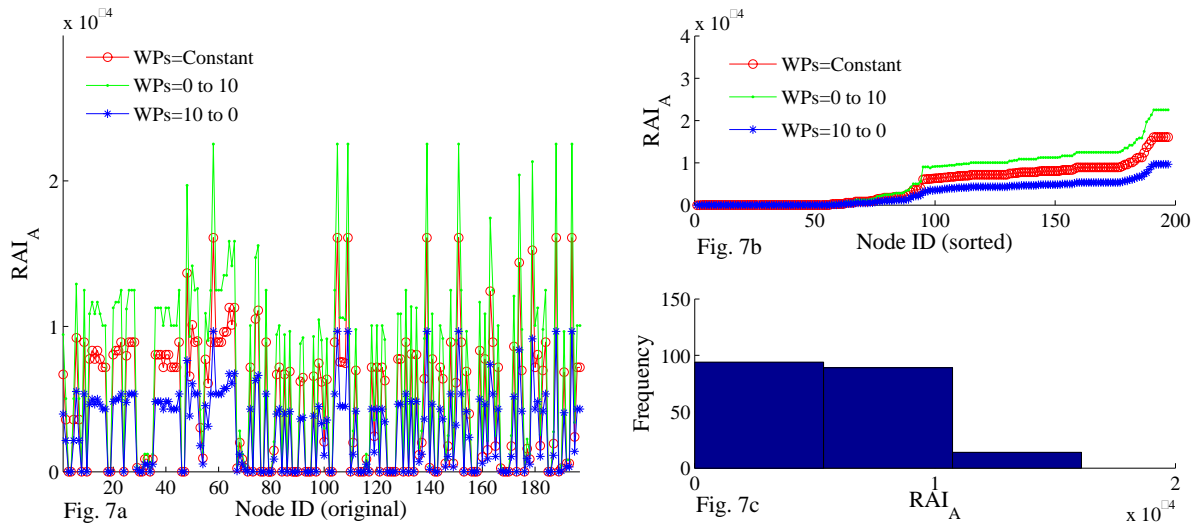
Ranking	Airport		Airspace (ACC)	
	RAI_P	Capacity	RAI_P	Capacity
1	WIEN SCHWECHAT	PARIS CDG	ROME	LONDON
2	ISTANBUL ATATURK	SCHIPHOL AMSTERDAM	PRESTWICK	MAASTRICHT
3	SCHIPHOL AMSTERDAM	KIEV BORISPOL	PARIS	KARLSRUHE
4	MADRID BARAJAS	MADRID BARAJAS	LANGEN	MUNICH
5	MUENCHEN 2	FRANKFURT	BUCHAREST	LONDON TC
6	COPENHAGEN KASTRUP	MUENCHEN 2	MUNICH	PARIS
7	OSLO GARDERMOEN	ROME/FIUMICINO	BREMEN	LANGEN
8	ANTALYA	LONDON HEATHROW	MADRID	ROME
9	KIEV BORISPOL	STOCKHOLM ARLANDA	ANKARA/IST ANBUL	MARSEILLE
10	HELSINKI-VANTAA	COPENHAGEN KASTRUP	BELGRADE	PRESTWICK

596 Table 2. Top ten airports and airspaces that have the highest RAI_P and capacities.

597
598

599 5.2.2. Relative area index with capacity reduction by absolute value (RAI_A)

600 The RAI_A is calculated by applying capacity reductions to each node by a certain
601 value (in flight per hour). We set the capacity reductions from 0 to 50 (flight per hour) to
602 examine the influences of absolute-value capacity reductions on network capacity. Similar to
603 the RAI_P case, three sets of weighting parameters are considered. The results of the RAI_A are
604 shown in Figure 7. A high correlation among the three sets of RAI_A is observed, with all the
605 correlation coefficients and Spearman’s rank correlation coefficients above 0.99, and the p -
606 values all close to zero. However, in contrast to RAI_P , no significant difference in the RAI_A
607 exists between the airport nodes and the ACC nodes (see Figure 7a). This is partially due to
608 the relatively small capacity reduction (by up to 50 flights per hour) such that most of the
609 airports and ACCs are far from being bottlenecked. Thus the global effects of flow reduction
610 induced by local degradation at airports or ACCs cannot be differentiated.



611 Figure 7. RAI_A in the European ATN. Fig. 7b is using new node IDs based on nodes sorted by their
612 RAI_A (with constant weighting parameters).
613

614 An interesting result of the RAI_A is shown when we sort all the nodes in an ascending
615 order with respect to RAI_A with constant weighting parameter (Figure 7b): The nodes can be
616 intuitively clustered into three groups according to their RAI_A , namely low (ID 1 - 95),
617 medium (ID 96 -180), and high (ID 181 - 195); see Figure 7b and Figure 7c.

618 Table 3 shows that the correlation between RAI_A and capacity is comparatively weak,
619 with only a few nodes in common in the top ten. The influence of a minor absolute capacity
620 reduction on the entire network is not in line with the magnitudes of the nodal capacities.
621

Ranking	Airport		Airspace (ACC)	
	RAI_A	Capacity	RAI_P	Capacity
1	WIEN SCHWECHAT	PARIS CDG	KYIV	LONDON
2	ATHINAI-E-VENIZELOS	SCHIPHOL AMSTERDAM	PRESTWICK	MAASTRICHT
3	ISTANBUL ATATURK	KIEV BORISPOL	NICOSIA	KARLSRUHE
4	ISTANBUL SABIHA	MADRID BARAJAS	BREMEN	MUNICH
5	MAKEDONIA	FRANKFURT	CANARIAS	LONDON TC
6	IZMIR ADNAN MENDERES	MUENCHEN 2	BUCHAREST	PARIS
7	ANTALYA	ROME/FIUMICINO	ROME	LANGEN
8	ANKARA ESENBOGA	LONDON HEATHROW	RIGA	ROME

9	MUENCHEN 2	STOCKHOLM ARLANDA	PARIS	MARSEILLE
10	CATANIA FONTANAROSSA	COPENHAGEN KASTRUP	STOCKHOLM	PRESTWICK

Table 3. Top ten airports and airspaces that have the highest RAI_A and capacities.

5.3. Comparison between BC and RAI

Given that the focus and the underlying assumptions of BC and RAI are different, it is difficult to conduct a direct comparison between these two robustness indices. Instead, we use relevant empirical data (ATFM delays) to examine the practical relevance of these two indices, and identify their strength and weakness.

Spearman's ranking correlation coefficient is used to reveal the relationships between the ranking of nodes based on the empirical data and the relevant robustness indices. Table 4 shows the correlation coefficients (r) among the six measures: the empirical ATFM delay, capacity, traffic load, RAI_P , RAI_A , and BC .

Measures		ATFM delay	Capacity	Traffic load	RAI_P	RAI_A	BC
ATFM delay	r	1.00	-0.44	0.23	-0.31	0.31	-0.12
	p	1.00	0.00	0.00	0.00	0.00	0.10
Capacity	r	-0.44	1.00	0.47	0.72	-0.24	0.37
	p	0.00	1.00	0.00	0.00	0.00	0.00
Traffic load	r	0.23	0.47	1.00	0.51	0.19	0.51
	p	0.00	0.00	1.00	0.00	0.01	0.00
RAI_P	r	-0.31	0.72	0.51	1.00	0.31	0.37
	p	0.00	0.00	0.00	1.00	0.00	0.00
RAI_A	r	0.31	-0.24	0.19	0.31	1.00	0.13
	p	0.00	0.00	0.01	0.00	1.00	0.06
BC	r	-0.12	0.37	0.51	0.37	0.13	1.00
	p	0.10	0.00	0.00	0.00	0.06	1.00

Table 4. Spearman's ranking correlation coefficients and the p -values among relevant indices and empirical data (ATFM delay)

Spearman's ranking correlation coefficient r between RAI_P and the traffic load is comparable with that between BC and the traffic load (0.51). Secondly, the ranking of the RAI_P is strongly correlated to the ranking of the nodal capacity (0.72), showing RAI_P to be an index more promising than BC to capture the nodal capacity. Thirdly, RAI_A has no meaningful correlation with any of the other indices. This indicates that the influence of a minor, absolute capacity reduction of a given node is not significantly related to traffic load, nodal capacity, or ATFM delays. However, we expect that when the absolute capacity reduction gets larger, say for a subset of the nodes that have large capacities, RAI_A is likely to provide a more meaningful characterization of the importance of nodes.

In Table 4, neither the RAI nor the BC captures the ATFM delays. This is explained by the fact that the ATFM delay is a result of a complex operational environment, involving multiple sectors and stakeholders; thus more sophisticated models are required to capture the ATFM delays in their entirety.

In order to further compare RAI and BC , we select the top 25 nodes with the highest ATFM delays¹, which are subsequently referred to as *bottlenecks*, and conduct a similar analysis restricted to these 25 bottlenecks. The findings are presented in Table 5. Here, BC again provides a poor performance with low Spearman's ranking correlation coefficient and high p -values. An important finding is that Spearman's ranking correlation coefficient

¹ These 25 nodes include 21 airports and 4 ACCs, with ATFM delays greater than the mean (3.9 minutes); see the Appendix for more information.

653 between RAI_A and RAI_P increases from 0.31 to 0.72, which means that the capacity
 654 reductions by percentage or absolute value have similar effects for these 25 nodes. In
 655 addition, both RAI_A and RAI_P better capture the ATFM delays at these bottlenecks, with $r =$
 656 0.44 and $r = 0.40$, respectively.

Measures		ATFM delay	Capacity	Traffic load	RAI_P	RAI_A	BC
ATFM delay	r	1.00	0.06	0.23	0.44	0.40	0.19
	p	1.00	0.78	0.28	0.03	0.05	0.36
Capacity	r	0.06	1.00	0.82	0.48	-0.03	0.22
	p	0.78	1.00	0.00	0.02	0.90	0.28
Traffic load	r	0.23	0.82	1.00	0.61	0.16	0.30
	p	0.28	0.00	1.00	0.00	0.45	0.15
RAI_P	r	0.44	0.48	0.61	1.00	0.72	0.38
	p	0.03	0.02	0.00	1.00	0.00	0.06
RAI_A	r	0.40	-0.03	0.16	0.72	1.00	0.23
	p	0.05	0.90	0.45	0.00	1.00	0.27
BC	r	0.19	0.22	0.30	0.38	0.23	1.00
	p	0.36	0.28	0.15	0.06	0.27	1.00

658 Table 5. Spearman's ranking correlation coefficients and the p -values among relevant indices and
 659 empirical data (ATFM delay), among the 25 high-ATFM-delay nodes.

660 6. Discussion

661 The commonly employed network robustness index, namely betweenness centrality
 662 (BC), reflects only the topological characteristics of the network, without taking into account
 663 traffic demand and nodal capacities. As a result, it can only capture traffic loads rather than
 664 capacity or ATFM delays, as we show in our results for the European air traffic network.
 665 Using BC as the robustness index of an ATN is quite limited in capturing the influence of
 666 local disruption on the network level, especially when the operational characteristics are
 667 within the purview of network operators.

668 Our finding that the BC is capable of capturing the actual traffic load at a particular
 669 node differs from that of Cats and Jenelius (2014), who found limited correlation between the
 670 passenger loads and BC s in a road network. We argue that this difference is caused by the
 671 different nature of road and air traffic. Compared to road users who are free to minimize their
 672 cost of travel by selecting alternative routes in a networks, aircrafts do not have the freedom
 673 to select alternative routes; instead, they fly along the routes in given flight plans and follow
 674 the guidance of air traffic control (ATC). In addition, the delay of air traffic often occurs at
 675 the departing airport as a result of air traffic management, while congestion and delays of
 676 road traffic take place en route. These differences imply that the BC may be an adequate
 677 indicator for air traffic volume in an ATN, since the shortest distance is an important factor in
 678 the design of flight plans.

679 The proposed robustness index (RAI) is more capable than the BC of capturing the
 680 importance of a given node in the event of capacity reduction, by considering traffic
 681 demands, actual flight paths, and nodal capacities, in addition to the topological features. It
 682 also encapsulates a range of scenarios involving different levels of capacity reductions,
 683 instead of simply removing a node or a link, which is typical in topological analysis leading
 684 up to BC and other indices. The concept and formulation of RAI is flexible enough to
 685 accommodate a wide range of cases involving different nature and severity of the capacity
 686 reduction. We first adopt the percentage-based capacity reduction in combination with a
 687 network flow maximisation technique for assessing the theoretical network capacity. We find
 688 that the RAI_P ranking at the aggregated nodes and ACCs are generally higher than those at
 689 the airport nodes. Although the use of three sets of weighting parameters results in different

690 rankings of nodes, the difference is extremely small. However, we note that the importance of
 691 the weighting parameters should be re-evaluated by introducing more sophisticated modelling
 692 elements, such as dynamic network modelling and routing and scheduling.

693 In addition to the percentage-based capacity reductions, we also applied the absolute
 694 capacity reduction to calculate RAI_A . This approach enables us to assess the influence of a
 695 certain event that causes absolute capacity reductions at given nodes. Unlike the RAI_P
 696 ranking, the result shows that the RAI_A ranking do not favour the high-capacity nodes such as
 697 the ACCs and aggregated nodes. In addition to the ranking, the RAI_A of the nodes in the
 698 European ATN can be intuitively categorized into three groups: High-, Medium- and Low-
 699 RAI_A nodes. A particular event such as sector- or runway-closure at the nodes in the High-
 700 RAI_A group will cause a greater impact on network capacity than if that event happens at the
 701 nodes in the Medium- and Low- RAI_A groups. This functionality provides the network
 702 management unit with a powerful tool to group and rank the critical nodes, not solely using
 703 the empirical delay data that may contain considerable inaccuracies. Compared to the BC,
 704 using the RAI is more flexible to assess network robustness (see RAI_P in Table 4 and RAI_A in
 705 Figure 7). Therefore, the proposed new index has the potential to be used to reflect the ranking
 706 of the constituent nodes in an ATN and to assess network robustness. Table 5 shows the
 707 superiority of RAI over BC at the 25 main bottlenecks.

708 There are potentially four extensions of this paper for future research. First, the
 709 formulation of the conventional index, BC can be improved to accommodate the features of
 710 air traffic, including traffic demands, flight routes and the heterogeneity between the airport
 711 and airspace nodes. Second, since the European ATN is not saturated and the capacity of
 712 each node varies dynamically, there is a need to capture network flows dynamically by
 713 introducing dynamic capacity constraints and flight times. Third, both the RAI_A and RAI_P
 714 require real data on the influence of capacity fluctuation on network capacity for their
 715 validation. This validation would enable the superiority of the RAI when compared to the
 716 current KPI of ATFM delays to be evaluated. Finally, unexpected events that occur in real-
 717 time, such as large-scale meteorological events and industrial action, may reduce the capacity
 718 at multiple airports and en-route airspace. Hence, any future analysis would benefit from an
 719 evaluation of the influence of capacity-reductions at multiple nodes in the network
 720 simultaneously, rather than at just a single node.

721 7. Conclusion

722 This paper proposes a new index, the RAI , to assess the robustness of the European
 723 ATN by calculating the influence of nodal capacity-reductions on network capacity. Using
 724 data from three of the busiest air traffic days in Europe in 2012, the RAI was assessed along
 725 topological index, the BC , as potential indicators for robustness. The results indicate that the
 726 RAI is better able to capture the importance of each node by taking into account not only the
 727 topological features, but also the traffic demands and the nodal capacities.

728 There are several potential operational applications of the RAI to air traffic
 729 management. Compared to ATFM delay that is the current indicator of network capacity and
 730 of any bottlenecks in the network, the RAI provides a detailed ranking of the nodes in the
 731 European ATN from the standpoint of any potential local degradation of capacity and its
 732 consequent impact on the overall network. Such a consideration has not been addressed by
 733 the ATFM delay, the BC or any other existing network performance indices for air traffic
 734 networks. RAI therefore provides a potentially powerful tool for the European ATM unit to
 735 identify and categorize the critical nodes in the network. This in turn can aid in improving
 736 network management and resource allocations, by identifying nodes with higher ‘marginal
 737 benefits’.

738 Given the expected rise in air traffic demand in Europe in the coming years, SESAR
739 is effectively revolutionising the nature of air traffic operations and their management in
740 Europe. However, as EUROCONTROL noted in their “Challenges for growth 2013”
741 (EUROCONTROL, 2013a), there is an urgent need to understand network performance in the
742 future European air traffic network and then to have appropriate metrics for this performance,
743 to a far greater degree of sophistication than the current ATFM delays. Given this need, we
744 recommend the use of the *RAI* methodology for the development of the future of European
745 network performance indicators.

746 **Acknowledgement**

747 The authors thank the EUROCONTROL for providing the data of flight profiles and
748 ATFM delays. We also thank Dr. Xiaoqian Sun who generously provided constructive
749 suggestions on network robustness.

750 **References**

- 751 Barrat, A., M. Barthelemy, R. Pastor-Satorras, & A. Vespignani. 2004. "The architecture of
752 complex weighted networks". *Proceedings of the National Academy of Sciences of*
753 *the United States of America*, 101(11), 3747-3752.
- 754 Brandes, U. 2001. "A faster algorithm for betweenness centrality*". *Journal of*
755 *Mathematical Sociology*, 25(2), 163-177.
- 756 Cats, O., & E. Jenelius. 2014. "Dynamic vulnerability analysis of public transport
757 networks: mitigation effects of real-time information". *Networks and Spatial*
758 *Economics*, 14(3-4), 435-463.
- 759 Dehmer, M. (2011). *Structural Analysis of Complex Networks*: Springer.
- 760 Di Paolo, E., K. Zhang, S. Yang, X.-B. Hu, & H. Liu. 2011. "Application of Complex Network
761 Theory and Genetic Algorithm in Airline Route Networks". *Transportation*
762 *Research Record: Journal of the Transportation Research Board*, 2214(-1), 50-58.
- 763 EUROCONTROL. (2007). *Capacity Assessment & Planning Guidance-An overview of the*
764 *European Network Capacity Planning Process*. Brussels, Belgium.
- 765 EUROCONTROL. (2013a). *Challenges of Growth 2013*. Brussels, Belgium.
- 766 EUROCONTROL. (2013b). *European Network Operations Plan 2013-2015*. Brussels,
767 Belgium.
- 768 EUROCONTROL. 2013c, "European Route Network Improvement Plan Part 2-European
769 ATS Route Network - Version 2013-2015", Brussels, Belgium.
- 770 EUROCONTROL. (2014). *Network Operations Report 2013*. Brussels, Belgium.
- 771 EUROCONTROL. (2015). *Seven-Year Flight Movements and Service Units Forecast: 2015-*
772 *2021*. Brussels, Belgium.
- 773 EUROCONTROL/FAA. (2009). *U.S./Europe Comparison of ATM-related Operational*
774 *Performance*.
- 775 Freeman, L. C. 1979. "Centrality in social networks conceptual clarification". *Social*
776 *networks*, 1(3), 215-239.
- 777 Geraci, A., F. Katki, L. McMonegal, B. Meyer, J. Lane, P. Wilson, . . . F. Springsteel. (1991).
778 *IEEE standard computer dictionary: Compilation of IEEE standard computer*
779 *glossaries*: IEEE Press.
- 780 Guimera, R., & L. A. N. Amaral. 2004. "Modeling the world-wide airport network". *The*
781 *European Physical Journal B-Condensed Matter and Complex Systems*, 38(2), 381-
782 385.
- 783 Holme, P., B. J. Kim, C. N. Yoon, & S. K. Han. 2002. "Attack vulnerability of complex
784 networks". *Physical Review E*, 65(5), 056109.
- 785 Holmes, B. J., Scott, John M. (2004). *Transportation network topologies*. Paper presented
786 at the Integrated Communications, Navigation, and Surveillance (ICNS)
787 Conference, Fairfax, Virginia, USA.
- 788 Holmgren, Å. J. (2007). A framework for vulnerability assessment of electric power
789 systems *Critical Infrastructure* (pp. 31-55): Springer.
- 790 Immers, B., I. Yperman, J. Stada, & A. Bleukx. 2004. "Reliability and robustness of
791 transportation networks: problem survey and examples". *Proceedings of the*
792 *NECTAR cluster meeting on reliability of networks, Amsterdam, the Netherlands*,
793 19-20.
- 794 Jahn, J. (2007). *Introduction to the theory of nonlinear optimization*: Springer.
- 795 Lordan, O., J. M. Sallan, P. Simo, & D. Gonzalez-Prieto. 2014. "Robustness of the air
796 transport network". *Transportation Research Part E: Logistics and Transportation*
797 *Review*, 68(0), 155-163.

- 798 Nagurney, A., & Q. Qiang. 2007a. "A network efficiency measure for congested
799 networks". *EPL (Europhysics Letters)*, 79(3), 38005.
- 800 Nagurney, A., & Q. Qiang. 2007b. "Robustness of transportation networks subject to
801 degradable links". *EPL (Europhysics Letters)*, 80(6), 68001.
- 802 Nagurney, A., & Q. Qiang. 2009. "A relative total cost index for the evaluation of
803 transportation network robustness in the presence of degradable links and
804 alternative travel behavior". *International Transactions in Operation Research*, 16,
805 49-67.
- 806 Newman, M. E. 2001. "Scientific collaboration networks. II. Shortest paths, weighted
807 networks, and centrality". *Physical Review E*, 64(1), 016132.
- 808 Pien, K.-C., A. Majumdar, K. Han, & W. Y. Ochieng. 2014. "A linear programming
809 approach to maximum flow estimation on the European air traffic network ". *in*
810 *the 6th International Conference on Research in Air Transportation (ICRAT2014)*,
811 2014: Istanbul Technical University, Turkey.
- 812 Sakakibara, H., Y. Kajitani, & N. Okada. 2004. "Road Network Robustness for Avoiding
813 Functional Isolation in Disasters". *Journal of Transportation Engineering*, 130(5),
814 560-567.
- 815 Scott, D. M., D. Novak, L. Aultman-Hall, & F. Guo. 2005. "Network robustness index- a
816 new method for identifying critical links and evaluating the performance of
817 transportation networks ". *Center for spatial analysis working paper*.
- 818 Sun, X., & S. Wandelt. 2014. "Network similarity analysis of air navigation route
819 systems". *Transportation Research Part E: Logistics and Transportation Review*,
820 70, 416-434.
- 821 Sun, X., S. Wandelt, & F. Linke. 2014. "Topological Properties of the Air Navigation Route
822 System using Complex Network Theory". *in the 6th International Conference on*
823 *Research in Air Transportation (ICRAT2014)*, 2014:Istanbul Technical University,
824 Turkey.
- 825 Wasserman, S. (1994). *Social network analysis: Methods and applications* (Vol. 8):
826 Cambridge university press.
- 827 Wei, P., L. Chen, & D. Sun. 2014. "Algebraic connectivity maximization of an air
828 transportation network: The flight routes' addition/deletion problem".
829 *Transportation Research Part E: Logistics and Transportation Review*, 61(0), 13-
830 27.
- 831 Zhao, C., B. Fu, & T. Wang. 2014. "Braess paradox and robustness of traffic networks
832 under stochastic user equilibrium". *Transportation Research Part E: Logistics and*
833 *Transportation Review*, 61(0), 135-141.
- 834

Appendix

The table below is concerned with the top 25 nodes in the European Air Traffic Network in terms of ATFM delays. Other performance indices of interest, including capacity, traffic load, *RAI* and *BC* are computed and presented for these 25 nodes, along with their rankings in each of the categories.

Nodes	Type	ID	ATFM delays		Capacity		Traffic		RAI				Betweenness		
			min/flt	ranking	flt/day	ranking	flt/day	ranking	RAI_P	ranking	RAI_A	ranking	BC	ranking	
1	BARCELONA	Airport	LEBL	18.74	1	1056	9	926	6	0.00191	6	0.00008	8	30	9
2	MUENCHEN 2	Airport	EDDM	12.32	2	1440	4	1060	4	0.00283	3	0.000092	2	0	11
3	PALMA-DE-MALLORCA	Airport	LEPA	11.78	3	992	10	836	7	0.00162	8	0.00008	9	0	11
4	WARSAWA OKECIE	Airport	EPWA	8.74	4	640	18	397	17	0.00016	24	0.000003	21	0	11
5	ALICANTE	Airport	LEAL	8.48	5	480	22	228	24	0.00088	14	0.00008	10	0	11
6	VALENCIA	Airport	LEVC	8.24	6	480	23	174	25	0.00088	15	0.00008	11	2226	3
7	BARCELONA	ACC	LECBCTA	7.78	7	3288	2	2893	2	0.00264	4	0.000009	19	397	5
8	NICOSIA	ACC	LCCCCTA	7.66	8	1200	6	976	5	0.00386	2	0.000161	1	380	6
9	ZURICH	Airport	LSZH	6.51	9	1152	7	788	9	0.00211	5	0.000089	3	0	11
10	GENEVE COINTRIN	Airport	LSGG	6.35	10	640	19	524	13	0.00126	12	0.000089	4	1439	4
11	NICE	Airport	LFMN	5.52	11	832	12	625	10	0.00159	9	0.000089	5	222	7
12	HERAKLION	Airport	LGIR	5.52	12	352	25	261	21	0.0006	21	0.000066	17	0	11
13	DUESSELDORF	Airport	EDDL	5.39	13	720	17	587	11	0.00061	20	0.000036	18	0	11
14	PALMA	ACC	LECPCTA	5.17	14	2208	3	1356	3	0.00646	1	0.00008	12	3575	1
15	BIRMINGHAM	Airport	EGBB	4.88	15	640	20	248	23	0.00101	13	0.000078	14	215	8
16	LONDON STANSTED	Airport	EGSS	4.68	16	800	14	411	16	0.00132	11	0.00008	13	0	11
17	MALAGA	Airport	LEMG	4.59	17	560	21	416	15	0.00088	16	0.000072	15	0	11
18	KARLSRUHE	ACC	EDMMCTA	4.5	18	7176	1	4301	1	0.00076	17	0	22	2782	2
19	PRAHA RUZYNE	Airport	LKPR	4.41	19	736	16	376	18	0.00163	7	0.000089	6	0	11
20	KOELN-BONN	Airport	EDDK	4.3	20	1280	5	288	20	0.0002	23	0	22	0	11
21	MILANO MALPENSA	Airport	LIMC	4.27	21	1120	8	562	12	0.00068	19	0.000009	20	0	11
22	HAMBURG	Airport	EDDH	4.18	22	768	15	372	19	0.00013	25	0	22	0	11
23	FERIHEGY BUDAPEST	Airport	LHBP	4.17	23	384	24	259	22	0.00074	18	0.000089	7	15	10
24	LONDON GATWICK	Airport	EGKK	4.06	24	960	11	797	8	0.00152	10	0.000072	16	0	11
25	TEGEL-BERLIN	Airport	EDDT	4.04	25	832	13	427	14	0.00023	22	0	22	0	11